

Article

MHD Flow of Nanofluid with Homogeneous-Heterogeneous Reactions in a Porous Medium under the Influence of Second-Order Velocity Slip

Fahd Almutairi ¹, S.M. Khaled ^{2,3,*} and Abdelhalim Ebaid ⁴

¹ Department of Chemical Engineering, Faculty of Engineering University of Tabuk, Tabuk 71491, Saudi Arabia; falmutairi@ut.edu.sa

² Department of Mathematics, Faculty of Sciences, Helwan University, Cairo 11795, Egypt

³ Department of Studies and Basic Sciences, Faculty of Community, University of Tabuk, Tabuk 71491, Saudi Arabia

⁴ Department of Mathematics, Faculty of Sciences, University of Tabuk, P.O. Box 741, Tabuk 71491, Saudi Arabia; aebaid@ut.edu.sa or halimgamil@yahoo.com

* Correspondence: ksmahmoud@ut.edu.sa; Tel.: +966-56-765-4109

Received: 25 January 2019; Accepted: 21 February 2019; Published: 26 February 2019



Abstract: The influence of second-order velocity slip on the MHD flow of nanofluid in a porous medium under the effects of homogeneous-heterogeneous reactions has been analyzed. The governing flow equation is exactly solved and compared with those in the literature for the skin friction coefficient in the absence of the second slip, where great differences have been observed. In addition, the effects of the permanent parameters on the skin friction coefficient, the velocity, and the concentration have been discussed in the presence of the second slip. As an important result, the behavior of the skin friction coefficient at various values of the porosity and volume fraction is changed from increasing (in the absence of the second slip) to decreasing (in the presence of the second slip), which confirms the importance of the second slip in modeling the boundary layer flow of nanofluids. In addition, five kinds of nanofluids have been investigated for the velocity profiles and it is found that the Ag-water nanofluid is the lowest. For only the heterogeneous reaction, the concentration equation has been exactly solved, while the numerical solution is applied in the general case. Accordingly, a reduction in the concentration occurs with the strengthening of the heterogenous reaction and also with the increase in the Schmidt parameter. Moreover, the Ag-water nanofluid is of lower concentration than the Cu-water nanofluid. This is also true for the general case, when both of the homogenous and heterogenous reactions take place.

Keywords: homogeneous-heterogeneous reactions; porous medium; first slip; second slip; exact solution

1. Introduction

The main characteristic of nanofluid is the significant enhancement of the thermal properties of the base fluid. The term nanofluid comes back to a pioneering experimental research by Choi [1] in which a conclusion had been reached that the thermal conductivity of a base fluid is enhanced up to two times by adding a small amount of nanoparticles. In addition, some authors [2,3] found that the dispersion of a small amount of copper nanoparticles led to 40% of the thermal conductivity of the fluid, while adding a small amount of carbon nanotubes in ethylene glycol or oil led to 50%. Aly and Ebaid [4] considered five metallic and nonmetallic nanoparticles in a base of water, where an effective approach was introduced to derive the exact solution. One of the important results in the

field of nanofluid flow has been presented by Majumder [5], in which it was experimentally proven that nanofluidic flow exhibits partial slip against the solid surface, which can be characterized by the so-called slip length. Accordingly, the authors in [6] discussed the effect of partial slip boundary condition on the flow and heat transfer of nanofluids past stretching sheet at constant wall temperature. Furthermore, the no-slip condition is no longer valid for fluid flows at the micro- and nanoscale and, instead, a certain degree of tangential slip must be allowed [7,8]. Very recently, Sharma and Ishak [9] studied the second-order velocity slip effect on the boundary layer flow of Cu-water-based nanofluid with heat transfer over a stretching sheet. Their numerical results were based on the finite element method (FEM). A model for isothermal homogeneous-heterogeneous reactions in boundary layer flow of viscous fluid past a flat plate was studied by Merkin [10]. He presented the homogeneous reaction by cubic autocatalysis and the heterogeneous reaction by a first-order process and showed that the surface reaction is the dominant mechanism near the leading edge of the plate. Chaudhary and Merkin [11] studied the homogenous-heterogeneous reactions in boundary layer flow of viscous fluid. They found the numerical solution near the leading edge of a flat plate. Bachok et al. [12] focused on the stagnation-point flow towards a stretching sheet with homogeneous-heterogeneous reactions effects. Effects of homogeneous-heterogeneous reactions on the flow of viscoelastic fluid towards a stretching sheet were investigated by Khan and Pop [13]. Kameswaran et al. [14] extended the work of [13] for nanofluid over a porous stretching sheet. In general, porous medium is used for transport and storage of energy. Analysis of flow through a porous medium has become the core of several scientific and engineering applications. These applications include the utilization of geothermal energy, the migration of moisture in fibrous insulation, food processing, casting and welding in manufacturing processes, the dispersion of chemical contaminants in different industrial processes, the design of nuclear reactors, chemical catalytic reactors, compact heat exchangers, solar power, and many others. Further, the use of micro/nano electromechanical systems (MEMS/NEMS) has been increased in many industries. Such systems have association with velocity slip [15–19]. Very recently, Hayat et al. [20] studied the MHD flow of nanofluid with homogeneous-heterogeneous reactions of two chemical species and velocity slip. In this field of research, some pioneer works were introduced in [21–24] in which several non-Newtonian models have been analyzed. In [21], a novel radiation MHD activation energy Carreau and nanofluid effects of thermal energy systems have been investigated. The combined electrical MHD Ohmic dissipation forced and free convection of an incompressible Maxwell fluid on a stagnation point heat and mass transfer energy conversion problem have been studied in [22]. In addition, an applied thermal system for heat and mass transfer and energy management problem of hydromagnetic flow with magnetic and viscous dissipation effects of micropolar nanofluids towards a stretching sheet has been investigated by [23]. Moreover, the effect of the slip boundary condition on the stagnation electrical MHD nanofluid mixed convection on a stretching sheet was introduced in [24].

The objective of this work is to extend the model investigated by Hayat et al. [20] by considering the second-order slip velocity. Therefore, the extended model is given as

$$f'''(\eta) = \left(\lambda + (1 - \phi)^{2.5} M \right) f'(\eta) - \phi_1 \left(f(\eta) f''(\eta) - (f'(\eta))^2 \right), \quad (1)$$

$$\frac{1}{Sc} g''(\eta) = Kg(\eta)(h(\eta))^2 - f(\eta)g'(\eta), \quad (2)$$

$$\frac{\delta}{Sc} h''(\eta) = -Kg(\eta)(h(\eta))^2 - f(\eta)h'(\eta), \quad (3)$$

subject to

$$f(0) = 0, f'(0) = 1 + \gamma f''(0) + \mu f'''(0), f'(\infty) = 0, \quad (4)$$

$$g'(0) = K_s g(0), g(\infty) = 1, \quad (5)$$

$$\delta h'(0) = -K_s g(0), h(\infty) = 0, \quad (6)$$

where

$$\phi_1 = (1 - \phi)^{2.5} \left(1 - \phi + \phi \frac{(\rho C_p)_s}{(\rho C_p)_f} \right), \tag{7}$$

and ϕ is the solid volume fraction of the nanoparticles, λ is the porosity parameter, M is the Hartman number, Sc is the Schmidt parameter, K is the measure of the strength of the homogeneous reaction, K_s is the measure of the strength of the heterogeneous reaction, δ is the ratio of the diffusion coefficient, ρ_s and ρ_f are respectively the densities of nanoparticles and base fluid, γ and μ are respectively the first and the second velocity slip parameters, and $f'(\eta)$, $g(\eta)$ and $h(\eta)$ are respectively the fluid velocity and the concentrations of the two chemical species.

Following [20], the parameter δ can be taken as unity especially when the diffusion coefficients of two chemical species are the same. In this case, we have [20]

$$h(\eta) + g(\eta) = 1, \tag{8}$$

and hence Equations (2) and (3) reduce to

$$\frac{1}{Sc} g''(\eta) = Kg(\eta)(1 - g(\eta))^2 - f(\eta)g'(\eta), \tag{9}$$

subject to the same boundary conditions given in Equation (5). In [20], the authors applied the homotopy analysis method to solve the set of boundary value problems (1)–(6) in the absence of the second slip parameter (i.e., when $\mu = 0$). However, Equation (1) with the boundary conditions (3) can be exactly solved, even in the presence of the second slip parameter μ , as will be introduced in the next section. This exact solution for $f(\eta)$ will be then compared with the results obtained by [20] at a special case. Further, this exact formula for $f(\eta)$ is to be inserted into Equation (9) to form with the boundary conditions (5) a single nonlinear differential equation in the unknown $g(\eta)$. Details of the suggested procedure are presented in the next section.

2. Methodology

Following [25,26], $f(\eta)$ can be obtained as

$$f(\eta) = \frac{1}{\beta(1 + \gamma\beta - \mu\beta^2)} \left(1 - e^{-\beta\eta} \right), \tag{10}$$

where β is the positive root of the following nonlinear equation:

$$\mu\beta^4 - \gamma\beta^3 - \left(1 + \lambda\mu + \mu M(1 - \phi)^{2.5} \right) \beta^2 + \left(\gamma\lambda + M\gamma(1 - \phi)^{2.5} \right) \beta + \left(\phi_1 + \lambda + M(1 - \phi)^{2.5} \right) = 0. \tag{11}$$

On inserting Equation (10) into Equation (9), we obtain the following nonlinear ordinary differential equation (ODE) for $g(\eta)$:

$$g''(\eta) + \Omega \left(1 - e^{-\beta\eta} \right) g'(\eta) - KScg(\eta)(1 - g(\eta))^2 = 0, \tag{12}$$

where Ω is defined as

$$\Omega = \frac{Sc}{\beta(1 + \gamma\beta - \mu\beta^2)}. \tag{13}$$

The skin friction coefficient is defined in [20] by Equation (14) and hence Equation (15) is obtained by using the exact expression for $f(\eta)$ in Equation (10).

$$\text{Skin friction coefficient} = -\frac{2}{(1 - \phi)^{2.5}} f''(0), \tag{14}$$

$$\text{Skin friction coefficient} = \frac{2\beta}{(1 - \phi)^{2.5}(1 + \gamma\beta - \mu\beta^2)}. \tag{15}$$

At the special case, $K \rightarrow 0$, the analytic solution of Equation (12) is given as

$$g(\eta) = \frac{1 + \varepsilon\Gamma(\Omega/\beta, \Omega/\beta e^{-\beta\eta}, \Omega/\beta)}{1 + \varepsilon\Gamma(\Omega/\beta, 0, \Omega/\beta)}, \tag{16}$$

where ε is defined by

$$\varepsilon = K_s(\beta)^{\Omega/\beta-1} \left(e^{\beta^2}/\Omega \right)^{\Omega/\beta}. \tag{17}$$

This case may be of a physical meaning when only the heterogenous reactions occur. The concentration is therefore given as

$$g(0) = \frac{1}{1 + \varepsilon\Gamma(\Omega/\beta, 0, \Omega/\beta)}. \tag{18}$$

3. Discussion

In the beginning, it should be noted that the exact formula for the skin friction coefficient given by Equation (15) will be invested here and used to validate the numerical results obtained in [20] by applying the homotopy analysis method (HAM) when the second slip vanishes (i.e., at $\mu = 0$). The thermophysical properties of water and nanoparticles are introduced in Table 1. These properties have been implemented to conduct the numerical results in Table 2. In view of these comparisons, it may be concluded that the outputs of [20] need some revisions, especially since the differences between the current exact values and the approximate ones seem to be obvious. Besides, the same values of the physical parameters [20] have been selected to hold these comparisons.

Table 1. Properties of water and nanoparticles.

	C_p (J/kg·K)	ρ (kg/m ³)	K (W/m·K)
Pure Water	4179	4179	0.613
Copper (Cu)	385	8933	401
Silver (Ag)	235	10500	429
Alumina (Al ₂ O ₃)	765	3970	40
Titanium Oxide(TiO ₂)	686.2	4250	8.9538
Silicon Dioxide (SiO ₂)	765	3970	36

Table 2. Comparisons between the numerical results of skin friction coefficient [20] and the present exact values for copper and silver at $\mu = 0$ and $\lambda = 0.4$.

ϕ	M	γ	Cu		Ag	
			HAM [20]	Exact (Present)	HAM [20]	Exact (Present)
0.05	0.5	1.0	1.278	1.23278	1.284	1.23843
0.1			1.465	1.41390	1.475	1.42485
0.2			1.955	1.88407	1.973	1.90636
0.2	0.1		1.897	1.81545	1.917	1.84209
	0.3		1.928	1.85097	1.945	1.87529
	0.7		1.981	1.91500	1.996	1.93552
	0.5	0.1	4.542	4.31610	4.672	4.45659
		0.5	2.827	2.70491	2.865	2.75469
		0.9	2.079	2.00347	2.098	2.02905

In the presence of the second slip, exact values for the skin friction coefficient for the Ag-water and the Cu-water nanofluids are listed in Table 3 at various values of ϕ , M , and γ when $\lambda = 0.4$.

The results reveal that the skin friction coefficient for both nanofluids increases with an increase in the volume fraction ϕ and the Hartman number M ; however, it decreases with the increase in the first slip γ and with the decrease in the second slip μ . Further, the variation of the skin friction coefficient is depicted in Figure 1 against the porosity parameter λ at various values of the solid volume fraction ϕ when $\mu = 0$. It is clear from this figure that the skin friction increases with increases in both λ and ϕ . However, in [20], it was found that this behavior is different than the current one. This also confirms the conclusion made above that the method applied in [20] needs further improvement. In addition, the results in Figure 2 indicate that the skin friction decreases with increases in both λ and ϕ in the presence of the second slip parameter. Therefore, the behavior is changed from increasing in Figure 1 ($\mu = 0$) to decreasing in Figure 2 ($\mu = -0.5$), which confirms the importance of the second slip in modeling the boundary layer flow of nanofluids.

Table 3. Values of skin friction coefficient for copper and silver at various values of ϕ , M , γ and μ at $\lambda = 0.4$.

ϕ	M	γ	μ	Cu	Ag
0.01	0.5	1.0	-0.5	0.83677	0.83698
0.03				0.85850	0.85891
0.05				0.92832	0.92930
0.02				0.1	0.83658
	0.3		0.84949	0.85013	
	0.7		0.86457	0.86483	
	0.5	0.1		1.37395	1.37485
		0.5		1.08412	1.08475
		0.9		0.89573	0.89618
		1.0	-0.1	1.06481	1.06653
			-0.5	0.85850	0.85891
			-0.9	0.72553	0.72545

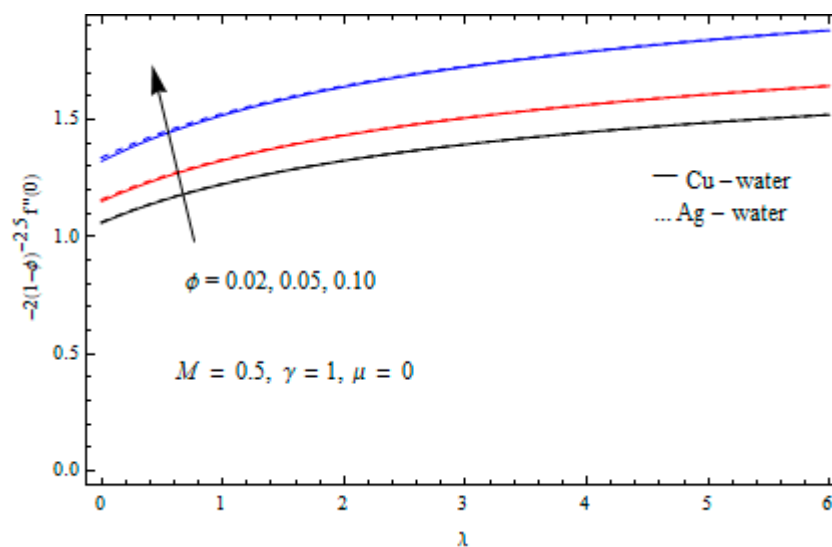


Figure 1. Effects of ϕ on skin friction coefficient when the second slip vanishes.

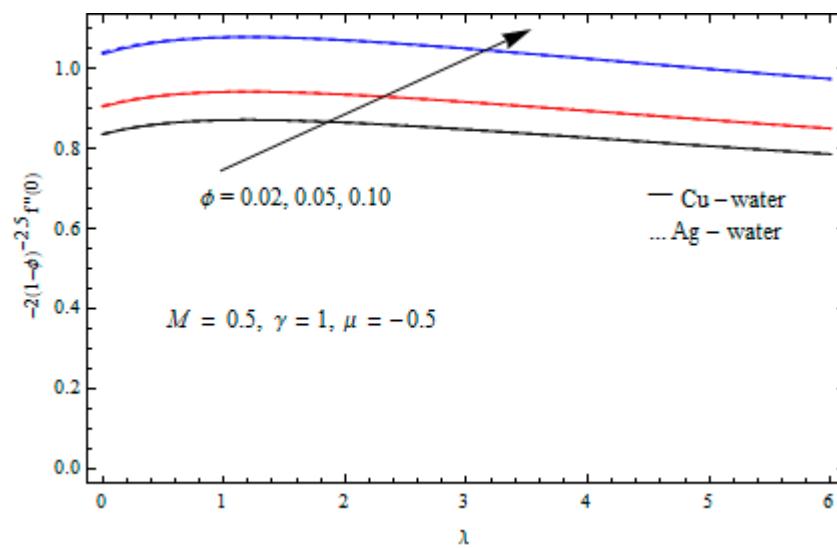


Figure 2. Effects of ϕ on skin friction coefficient in the presence of second slip.

The effect of the first slip parameter γ on the velocity of the nanofluids suspended with five nanoparticles is displayed through Figures 3–5. Figures 3 and 4 show that the velocities of the Ag/Cu/TiO₂-water nanofluids satisfy $f'(\eta)|_{Ag} < f'(\eta)|_{Cu} < f'(\eta)|_{TiO_2}$. Figure 5 indicates that $f'(\eta)|_{SiO_2} \approx f'(\eta)|_{Al_2O_3} \approx f'(\eta)|_{TiO_2}$. Therefore, it can be concluded from Figures 3–5 that the Ag-water nanofluid is of lower velocity than any of the four other types. This later conclusion is also observed and confirmed through Figures 6–8 for the effect of the second slip μ on the velocity of the present five types of nanofluids.

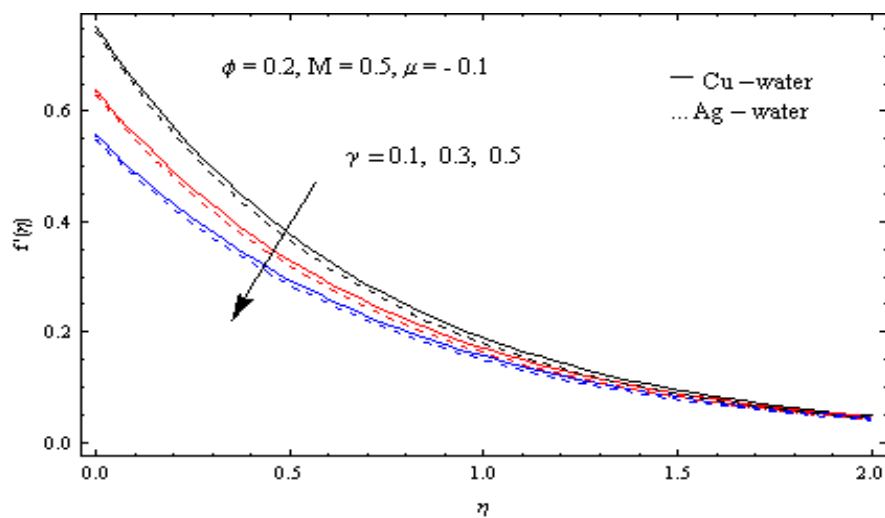


Figure 3. Effect of first slip γ on velocity of Cu-water and Ag-water nanofluids.

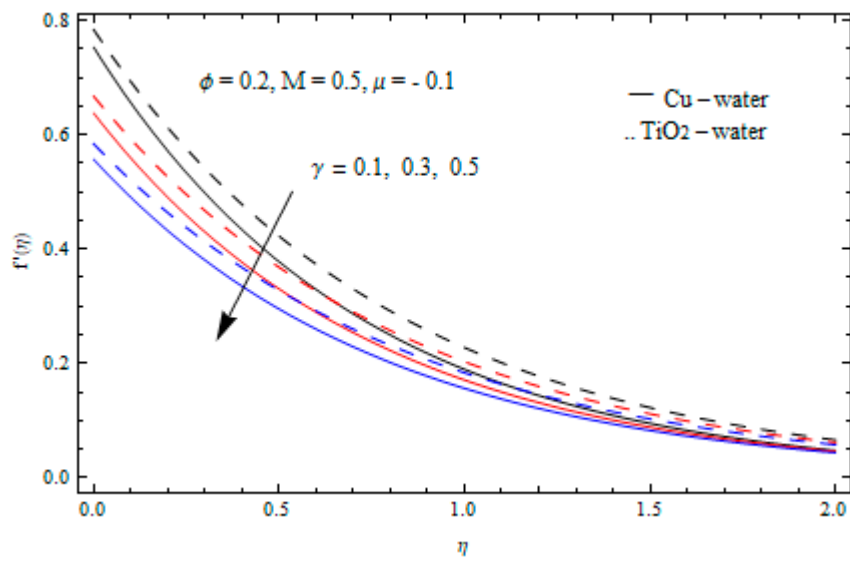


Figure 4. Effect of first slip γ on velocity of Cu-water and TiO₂-water nanofluids.

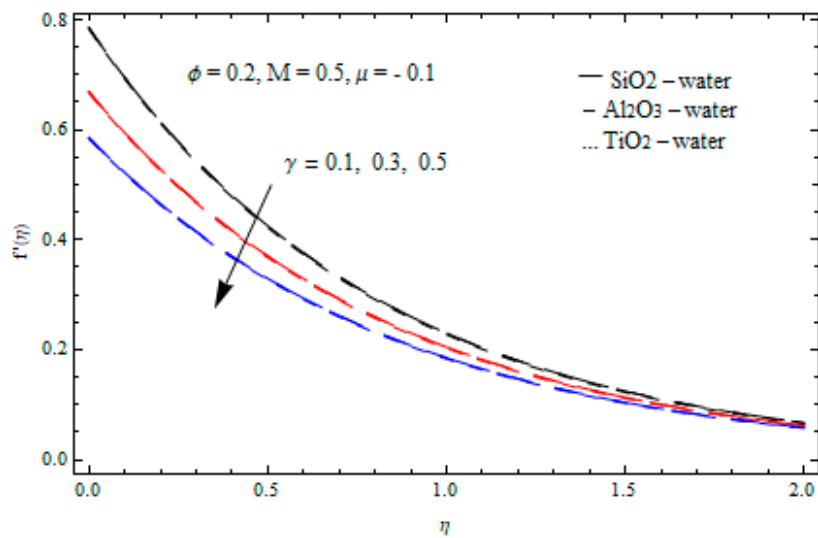


Figure 5. Effect of first slip γ on velocity of SiO₂-water, Al₂O₃-water, and TiO₂-water nanofluids.

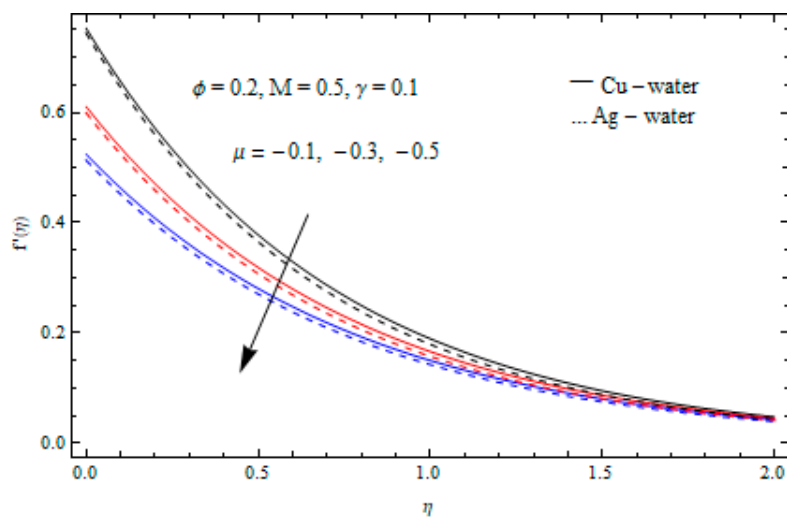


Figure 6. Effect of second slip μ on velocity of Cu-water and Ag-water nanofluids.

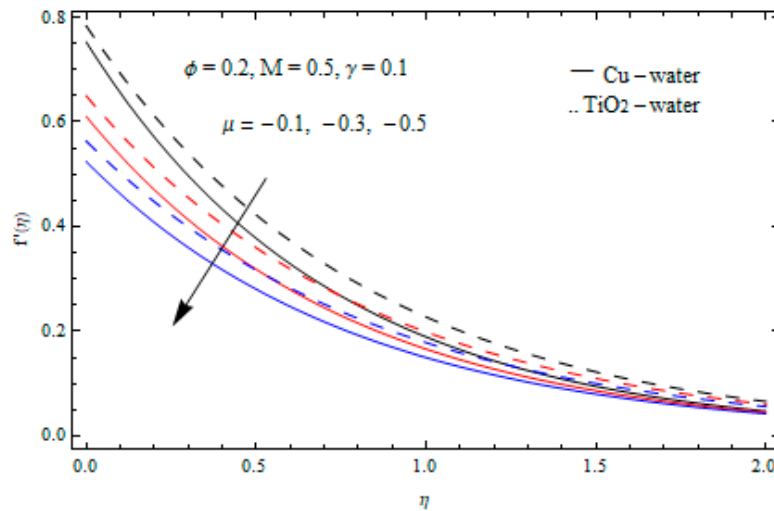


Figure 7. Effect of second slip μ on velocity of Cu-water and TiO₂-water nanofluids.

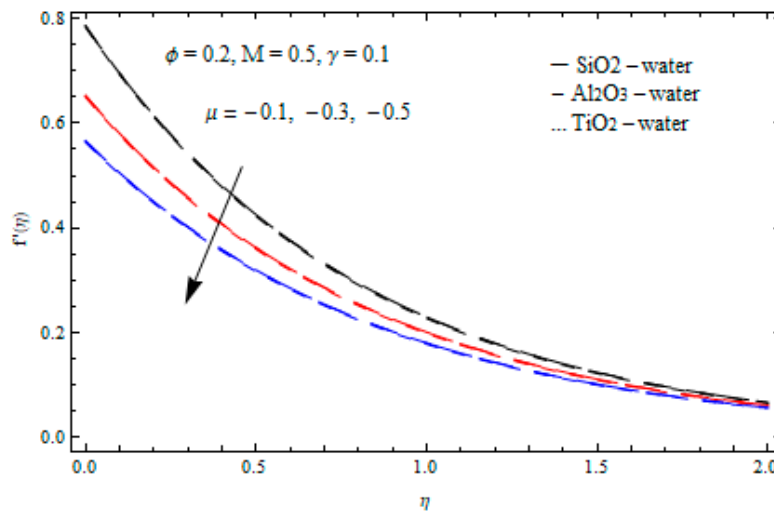


Figure 8. Effect of second slip μ on velocity of SiO₂-water, Al₂O₃-water, and TiO₂-water nanofluids.

In the absence of the homogenous reaction (i.e., at $K = 0$), the exact solution for the concentration $g(\eta)$ is available and given by Equation (16). In that case, the effects of K_s and Sc on $g(\eta)$ are plotted in Figures 9 and 10, respectively. It is shown that a reduction in the concentration occurs with the strengthening of the heterogenous reaction K_s and also with the increase in the Schmidt parameter Sc . Moreover, the Ag-water nanofluid is of lower concentration than the Cu-water nanofluid. This is also true for the general case, when both of the homogenous and heterogenous reactions take place in Figure 11, where the NDSolve command in Mathematica 7.0 (Wolfram Research, Champaign, IL, USA) has been used to solve the systems (5) and (12).

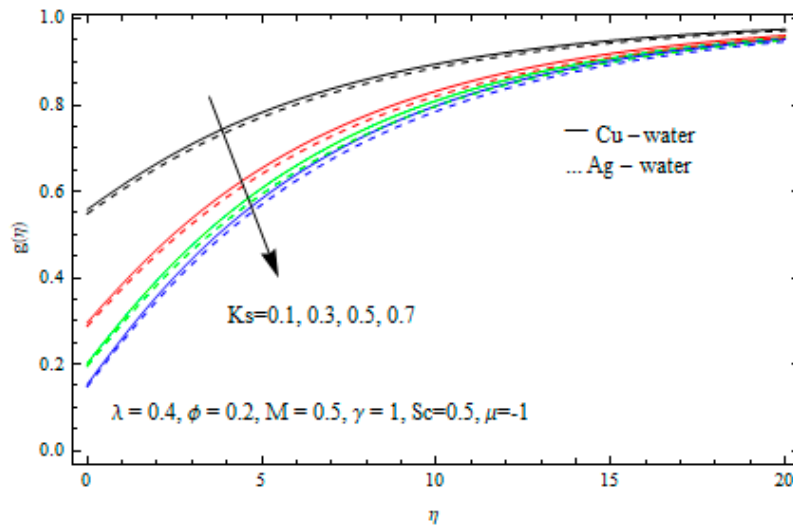


Figure 9. Effects of K_s on g at $K = 0$.

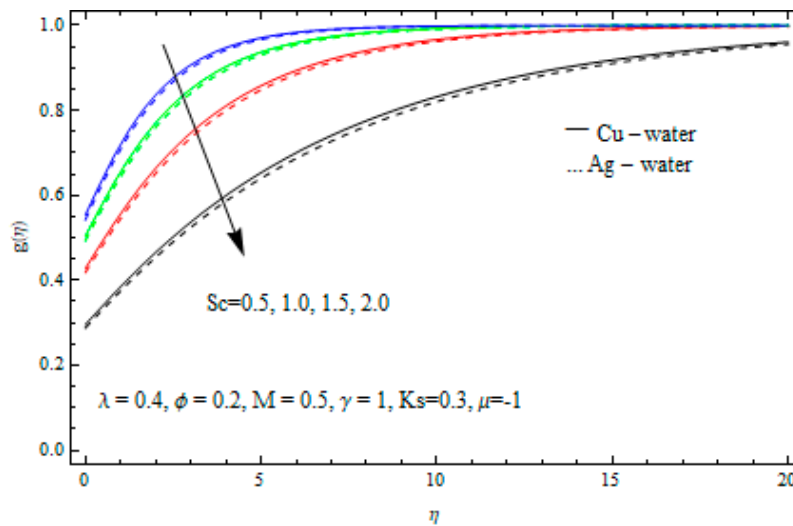


Figure 10. Effects of Sc on g at $K = 0$.

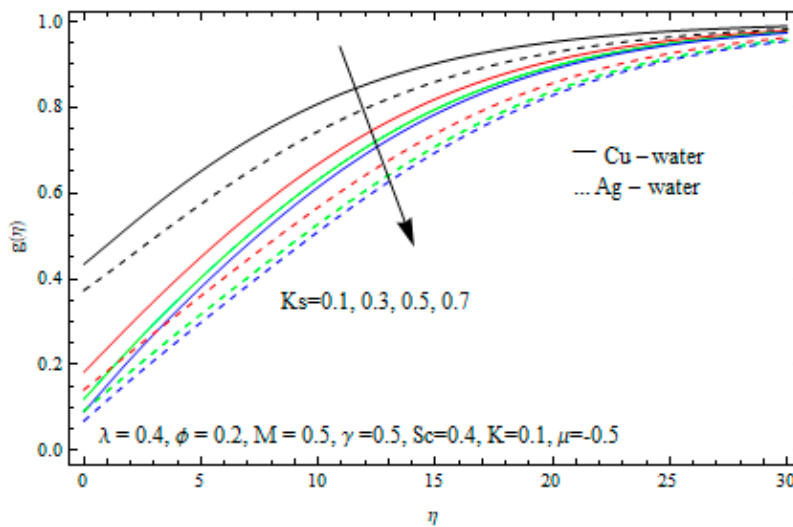


Figure 11. Effects of K_s on g .

4. Conclusions

In this paper, the effect of second velocity slip on the MHD flow of nanofluid in a porous medium with homogeneous-heterogeneous reactions has been analyzed. In the absence of the second slip, remarkable differences have been detected between the current exact results and those in the literature for the skin friction coefficient. For velocity, it has been found that the Ag-water nanofluid is lower than the other four kinds of nanofluids. For concentration, the exact solution has been given when only the heterogeneous reaction occurs. When both of the homogenous and heterogenous reactions take place, the concentration equation has been numerically solved. The concentration reduces with the strengthening of the heterogenous reaction and also with the increase in the Schmidt parameter, where the Ag-water nanofluid is of lower concentration than the Cu-water nanofluid.

Author Contributions: Conceptualization, F.A. and S.M.K.; methodology, F.A.; software, A.E.; validation, A.E.; project administration, F.A.; funding acquisition, F.A.

Funding: This research was funded by the Deanship of Scientific Research (DSR), University of Tabuk, Tabuk, Saudi Arabia, grant number 0074-1439-S.

Conflicts of Interest: The authors declare no conflict of interest.

References

- Choi, S.U.S. Enhancing thermal conductivity of fluids with nanoparticles. In *Developments and Applications of Non-Newtonian Flows*; Siginer, D.A., Wang, H.P., Eds.; ASME: New York, NY, USA, 1995; Volume 66, pp. 99–105.
- Eastman, J.A.; Choi, S.U.S.; Li, S.; Yu, W.; Thompson, L.J. Anomalously increased effective thermal conductivity of ethylene glycol-based nanofluids containing copper nanoparticles. *Appl. Phys. Lett.* **2001**, *78*, 718–720. [[CrossRef](#)]
- Choi, S.U.S.; Zhang, Z.G.; Yu, W.; Lockwoow, F.E.; Grulke, E.A. Anomalous thermal conductivities enhancement on nanotube suspension. *Appl. Phys. Lett.* **2001**, *79*, 2252–2254. [[CrossRef](#)]
- Aly, E.H.; Ebaid, A. Exact analytical solution for suction and injection flow with thermal enhancement of five nanofluids over an isothermal stretching sheet with effect of the slip model: A comparative study. *Abstr. Appl. Anal.* **2013**, *2013*, 721578. [[CrossRef](#)]
- Majumder, M.; Chopra, N.; Andrews, R.; Hinds, B.J. Nanoscale hydrodynamics: Enhanced flow in carbon nanotubes. *Nature* **2005**, *438*, 44–46. [[CrossRef](#)] [[PubMed](#)]
- Noghrehabadi, A.; Pourrajab, R.; Ghalambaz, M. Effect of partial slip boundary condition on the flow and heat transfer of nanofluids past stretching sheet prescribed constant wall temperature. *Int. J. Sci.* **2012**, *54*, 253–261. [[CrossRef](#)]
- Gad-el-Hak, M. The fluid mechanics of macrodevices—the Freeman scholar lecture. *J. Fluids Eng.* **1999**, *121*, 5–33. [[CrossRef](#)]
- Van Gorder, R.A.; Sweet, E.; Vajravelu, K. Nano boundary layers over stretching surfaces. *Commun. Nonlinear Sci. Numer. Simulat.* **2010**, *15*, 1494–1500. [[CrossRef](#)]
- Sharma, R.; Ishak, A. Second order slip flow of Cu-water nanofluid over a stretching sheet with heat transfer. *Wseas Trans. Fluid Mech.* **2014**, *9*, 26–33.
- Merkin, J.H. A model for isothermal homogeneous-heterogeneous reactions in boundary layer flow. *Math. Comput. Model.* **1996**, *24*, 125–136. [[CrossRef](#)]
- Chaudhary, M.A.; Merkin, J.H. A simple isothermal model for homogeneous-heterogeneous reactions in boundary layer flow: I. Equal diffusivities. *Fluid Dyn. Res.* **1995**, *16*, 311–333. [[CrossRef](#)]
- Bachok, N.; Ishak, A.; Pop, I. On the stagnation-point flow towards a stretching sheet with homogeneous-heterogeneous reactions effects. *Commun. Nonlinear Sci. Numer. Simul.* **2011**, *16*, 4296–4302. [[CrossRef](#)]
- Khan, W.A.; Pop, I. Effects of homogeneous-heterogeneous reactions on the viscoelastic fluid towards a stretching sheet. *J. Heat Transf.* **2012**, *134*, 1–5. [[CrossRef](#)]
- Kameswaran, P.K.; Shaw, S.; Sibanda, P.; Murthy, P.V.S.N. Homogeneous-heterogeneous reactions in a nanofluid flow due to porous stretching sheet. *Int. J. Heat Mass Transf.* **2013**, *57*, 465–472. [[CrossRef](#)]

15. Rashidi, M.M.; Kavyani, M.; Abelman, S. Investigation of entropy generation in MHD and slip flow over a rotating porous disk with variable properties. *Int. J. Heat Mass Transf.* **2014**, *70*, 892–917. [[CrossRef](#)]
16. Mahmoud, M.A.A.; Waheed, S.E. MHD flow and heat transfer of a micropolar fluid over a stretching surface with heat generation (absorption) and slip velocity. *J. Egypt. Math. Soc.* **2012**, *20*, 20–27. [[CrossRef](#)]
17. Ibrahim, W.; Shankar, B. MHD boundary layer flow and heat transfer of a nanofluid past a permeable stretching sheet with velocity, thermal and solutal slip boundary conditions. *Comput. Fluids* **2013**, *75*, 1–10. [[CrossRef](#)]
18. Rooholghdos, S.A.; Roohi, E. Extension of a second order velocity slip/temperature jump boundary condition to simulate high speed micro/nanoflows. *Comput. Math. Appl.* **2014**, *67*, 2029–2040. [[CrossRef](#)]
19. Malvandi, A.; Ganji, D.D. Brownian motion and thermophoresis effects on slip flow of alumina/water nanofluid inside a circular microchannel in the presence of a magnetic field. *Int. J. Therm. Sci.* **2014**, *84*, 196–206. [[CrossRef](#)]
20. Hayat, T.; Imtiaz, M.; Alsaedi, A. MHD flow of nanofluid with homogeneous-heterogeneous reactions and velocity slip. *Therm. Sci.* **2017**, in press. [[CrossRef](#)]
21. Hsiao, K.-L. To Promote Radiation Electrical MHD Activation Energy Thermal Extrusion Manufacturing System Efficiency by Using Carreau-Nanofluid with Parameters Control Method. *Energy* **2017**, *130*, 486–499. [[CrossRef](#)]
22. Hsiao, K.-L. Combined Electrical MHD Heat Transfer Thermal Extrusion System Using Maxwell Fluid with Radiative and Viscous Dissipation Effects. *Appl. Therm. Eng.* **2016**. [[CrossRef](#)]
23. Hsiao, K.-L. Micropolar Nanofluid Flow with MHD and Viscous Dissipation Effects towards a Stretching Sheet with Multimedia Feature. *Int. J. Heat Mass Transf.* **2017**, *112*, 983–990. [[CrossRef](#)]
24. Hsiao, K.-L. Stagnation Electrical MHD Nanofluid Mixed Convection with Slip Boundary on a Stretching Sheet. *Appl. Therm. Eng.* **2016**, *98*, 850–861. [[CrossRef](#)]
25. Ebaid, A.; al Mutairi, F.; Khaled, S.M. Effect of velocity slip boundary condition on the flow and heat transfer of Cu-Water and TiO₂-Water Nanofluids in the Presence of a Magnetic Field. *Adv. Math. Phys.* **2014**, *2014*, 538950. [[CrossRef](#)]
26. Ebaid, A.; al Sharif, M.A. Application of Laplace Transform for the Exact Effect of a Magnetic Field on Heat Transfer of Carbon Nanotubes-Suspended Nanofluids. *Z. Für Nat. A* **2015**, *70*, 471–475. [[CrossRef](#)]



© 2019 by the authors. Licensee MDPI, Basel, Switzerland. This article is an open access article distributed under the terms and conditions of the Creative Commons Attribution (CC BY) license (<http://creativecommons.org/licenses/by/4.0/>).